JOURNAL OF GEOPHYSICAL RESEARCH, VOL. 102, NO. A2, PAGES 2381-2390, FEBRUARY 1, 1997

Multiple-timescales analysis of ideal poloidal Alfvén waves

Ian R. Mann

Astronomy Unit, Department of Mathematical Sciences, Queen Mary and Westfield College, London

Andrew N. Wright [1] and Alan W. Hood

Department of Mathematical and Computational Sciences, University of St. Andrews, Fife Scotland

Abstract.
Time-dependent analytic solutions for the evolution of undriven ideal standing poloidal Alfvén waves are considered in a box model magnetosphere. Assuming an "azimuthal" variation of $\exp i\lambda y$, where λ is large, we use the asymptotic method of multiple timescales to determine analytic solutions over the long timescale σ defined by $\sigma = \epsilon t$, where $\epsilon = 1/\lambda$. Our asymptotic poloidal Alfvén wave solutions (with $\lambda \gg k_x, k_z$) accurately reproduce the undriven ideal wave polarization rotation from poloidal to toroidal in time determined numerically by *Mann and Wright* [1995]. Using the same asymptotic method, we further consider the evolution of radially localized large λ Alfvén waves. We find that undriven waves having k_x, $\lambda \gg k_z$, oscillating in a radially inhomogeneous plasma remain incompressible to leading order and experience similar asymptotically toroidal behavior as $t \to \infty$. Consequently, undriven poloidal Alfvén waves and, in general, transversally localized large λ ideal Alfvén wave disturbances have a finite lifetime before they evolve into purely decoupled toroidal Alfvén waves. This polarization rotation may be apparent in waves driven by the drift-bounce resonance mechanism in situations where the wave evolution occurs more rapidly than ionospheric damping. This can be possible on the dayside of the magnetosphere, with the evolution more likely to be observable toward the end of a temporal wave packet when the driving mechanism is no longer operative.

1. Introduction

Understanding the time-dependent evolution of ultralow frequency (ULF) hydromagnetic waves is important when trying to identify pulsation energy sources and when interpreting both ground-based and satellite data. ULF waves with quasi-sinusoidal wave trains have historically been classified according to their oscillation period. More recent studies [e.g., *Kokubun et al.*, 1989] have highlighted the importance of analyzing wave polarizations when trying to identify wave energy sources. ULF pulsations may be driven by sources which are either internal or external to the magnetosphere.

Early work on the external excitation of pulsations considered the possibility of coupling solar wind excited Kelvin-Helmholtz magnetopause surface waves to localized field line resonances (FLRs) at positions where the local Alfvén eigenfrequency matched the frequency of the surface wave [e.g., *Chen and Hasegawa*, 1974; *Southwood*, 1974]. Later treatments considered the excitation of magnetospheric cavity/waveguide modes which could themselves excite FLRs where their frequencies matched local Alfvén eigenfrequencies [e.g., *Kivelson and Southwood*, 1985, 1986]. These external sources resonantly excite essentially Alfvénic waves having low azimuthal wavenumbers ($m < 10$) which are dominantly toroidally (azimuthally) polarized.

Several other excitation mechanisms have been proposed which can extract free energy from internal magnetospheric plasma configurations, such as the drift-mirror instability [*Hasegawa*, 1969] and ballooning instabilities [e.g., *Chan et al.*, 1994]. Free energy can also be extracted from energetic particle populations, for example, through the drift-bounce resonance mechanism [*Southwood et al.*, 1969; *Southwood*, 1976; *Chen and Hasegawa*, 1988]. Depending upon the local plasma configurations, both mechanisms may sometimes be operative, resulting in, for example, the coupled drift-Alfvén-ballooning-mirror (DABM) instability discussed by *Chen and Hasegawa* [1991].

[1] On leave at National Institute of Water and Atmospheric Research Ltd., Kilbirnie, Wellington, New Zealand.

Paper number 96JA03034.
0148-0227/97/96JA-03034$09.00

In this paper we consider the temporal evolution of large m radially polarized transverse Pc4-5 pulsations (classified as R class waves by *Kokubun et al.* [1989]) which may have been excited by drift-bounce resonance with energetic protons. Waves driven by this mechanism are expected to be dominantly radially polarized, with the instability favoring large m and low frequencies [*Southwood*, 1976]. The lowest frequency standing waves which are unstable are second harmonic [see, e.g., *Southwood and Kivelson*, 1982], and this may explain the observations reported by *Takahashi and McPherron* [1984] of the predominance of the second harmonic in observations of radially polarized afternoon Pc4 waves.

Detailed satellite observations of these Alfvénic radially polarized waves show them to occur during periods of quiet geomagnetic activity, at all local times, with a maximum occurrence in the afternoon and a minimum occurrence between 0400 and 1100 magnetic local time (MLT) [*Anderson et al.*, 1990; *Kokubun et al.*, 1989; *Takahashi and McPherron*, 1984]. They typically occur when $L < 7$ around noon, increasing with local time to have $L > 7$ at midnight [*Anderson et al.*, 1990]. Waves can be extended in longitude, typically $\sim 1.5 - 8.0$ hours in MLT [*Engebretson et al.*, 1992] and are strongly localized in latitide with observed equatorial widths $\sim 0.2 - 1.6\ R_E$ by *Singer et al.* [1982], and a range of $0.2 - 3.1\ R_E$ (with a mean of $1.2\ R_E$) in 21 events reported by *Engebretson et al.* [1992].

Despite their broad longitudinal extent, multiple satellite observations of poloidal Alfvén waves often show high incoherencies between adjacent satellites. This implies large azimuthal wavenumbers, typically $m \sim 100$ [*Hughes et al.*, 1978b]. Detailed examination of particle behavior in the presence of poloidal Alfvén waves by *Takahashi et al.* [1990] confirmed azimuthal wavenumbers $m \sim 100$, found westward phase propagation, and concluded the waves had been driven by drift-bounce resonance with ~ 100-keV protons. Other studies have also found evidence for Pc4-5 poloidal Alfvén waves being driven by bounce resonance with energetic protons [*Hughes et al.*, 1978a, b; *Singer et al.*, 1982; *Hughes and Grard*, 1984; *Takahashi and McPherron*, 1984; *Engebretson et al.*, 1988; *Kokubun et al.*, 1989; *Anderson et al.*, 1990; *Engebretson et al.*, 1992].

Giant pulsations (Pgs) are a subset of radially polarized Pc4 waves, with similar properties to the poloidal Alfvén waves discussed above. Their occurrence, however, is limited to the early morning, with the waves characterized by smaller (but still large) azimuthal wavenumbers (typically $m \sim 20 - 40$). Pgs are also strongly radially localized (with typical equatorial widths $\sim 1\ R_E$), are observed during quiet times, and have extremely sinusoidal ground magnetometer signals [*Rostoker et al.*, 1979; *Glassmeier*, 1980; *Hillebrand et al.*, 1982; *Poulter et al.*, 1983; *Chisham et al.*, 1990; *Takahashi et al.*, 1992]. Poloidal Alfvén waves, by virtue of their larger azimuthal wavenumbers and hence finer-scale ionospheric variations, are believed to be screened from ground-based magnetometers [*Hughes and Southwood*, 1976; *Takahashi et al.*, 1992]. Pgs may also be driven by the drift-bounce resonance mechanism [*Glassmeier*, 1980; *Chisham et al.*, 1992; *Chisham*, 1996].

Compressional storm-time Pc5 waves are also believed to be driven by westward drifting energetic particles; however, they are not the subject of this paper. Storm-time Pc5s are thought to be driven by particles injected during substorms, whereas the poloidal Alfvén waves we consider are essentially incompressible and appear to be driven some time after injection during quiet geomagetic periods characterized by low convection electric fields but perhaps during periods of enhanced ring current [*Anderson et al.*, 1991]. As suggested by *Engebretson et al.* [1992], since the DABM instability is stabilized by 1-keV ions [*Chen and Hasegawa*, 1991], poloidal Alfvén waves are perhaps only excited once the low-energy particle population has decayed, allowing the higher-energy ~ 100-keV protons to drive the waves.

Despite being dominantly radially polarized, transverse poloidal Alfvén waves observed in the magnetosphere (and Pgs observed from the ground) are often associated with a significant azimuthal component [e.g., *Takahashi and Anderson*, 1992]. Whilst these waves are consistent with the guided poloidal mode discussed by *Radoski* [1967], the existence of the toroidal component has in the past been interpreted as a coupling between the poloidal and toroidal modes. As shown in time-dependent numerical studies by *Mann and Wright* [1995], an initially poloidally polarized Alfvén wave oscillating in a radially inhomogeneous plasma experiences a polarization rotation from poloidal to toroidal in time due to phase mixing. Hence the existence of both poloidal and toroidal components in high-m wave observations could be attributed to evolution of the wave fields in time.

In this paper we present multiple-timescales analytic solutions for undriven high-m poloidal Alfvén waves in fully compressible inhomogeneous MHD plasmas. We compare our analytic solutions to numerical results and examine the importance of the radial localization of poloidal Alfvén waves in the solution to the initial value problem. The paper is structured as follows: section 2 describes the governing equations and examines the relevant orderings of wave parameters; section 3 computes the multiple-timescales wave solutions; section 4 considers the characteristics of azimuthally standing and traveling waves; and section 5 compares our analytic solutions to numerical results. Section 6 compares our results to other high-m Alfvén wave studies and to observations, and finally, section 7 concludes and summarizes our paper.

2. Governing Equations and Wave Variable Orderings

We consider the evolution of MHD waves in a one-dimensional box model for the magnetosphere [e.g., *Southwood*, 1974]. We assume a uniform background

magnetic field ($\mathbf{B} = B_0\hat{\mathbf{z}}$), introduce a transverse Alfvén speed gradient by prescribing $\rho(x)$, and assume a perfectly conducting ionosphere. We consider a low-β plasma (where β is the ratio of thermal/magnetic pressure), and solve for the plasma displacements

$$\xi = (\xi_x(x,t), \xi_y(x,t), 0)e^{i\lambda y} \sin k_z z. \quad (1)$$

The waves are periodic in $\hat{\mathbf{y}}$ (analogous to azimuth in a dipole) and are standing in $\hat{\mathbf{z}}$, having wavenumbers λ and k_z, respectively. The wavenumber $\lambda \gg k_z$ throughout this study.

Within this model, linear MHD waves can be described by the following coupled (and normalized) differential equations

$$\frac{1}{\omega_A^2(x)}\frac{\partial^2 \xi_x}{\partial t^2} + \xi_x = -\frac{1}{k_z^2}\frac{\partial b_z}{\partial x} \quad (2)$$

$$\frac{1}{\omega_A^2(x)}\frac{\partial^2 \xi_y}{\partial t^2} + \xi_y = -\frac{i}{k_z^2}\lambda b_z \quad (3)$$

$$b_z = -\frac{\partial \xi_x}{\partial x} - i\lambda\xi_y \quad (4)$$

where $\omega_A(x)$ is the local Alfvén frequency defined by $\omega_A^2(x) = k_z^2 v_A^2(x)$. Lengths are normalized with respect to the depth of the box (L_x), magnetic fields by B_0, and densities by ρ_0 in the center of the box. Time is normalized with respect to $T_N = L_x/V_N$, where V_N is the normalizing Alfvén speed ($V_N = B_0/\sqrt{\mu_0\rho_0}$).

Equations (2) and (3) can be considered to describe poloidal and toroidal Alfvén waves, coupled by the (linear) compressional magnetic field component b_z. Since we consider waves with large λ it is instructive to investigate wave variable orderings in this limit.

2.1. Poloidal Alfvén Waves ($\lambda \gg \partial/\partial x, k_z$)

As discussed by *Mann and Wright* [1995], when azimuthal wave variations are more rapid than those in either the radial ($\hat{\mathbf{x}}$) or field aligned ($\hat{\mathbf{z}}$) directions (i.e., $\lambda \gg \partial/\partial x, k_z$), the following ordering exists. From our normalization $v_A \sim O(1)$, and hence (3) implies that for $k_z \sim O(1)$ then $\xi_y \sim \dot{\xi}_y$ and hence $b_z \sim \xi_y/\lambda$. Consequently, the left-hand side of (4) is $\sim \xi_y/\lambda$, which must be much less than the right-hand side of (4) when λ is large. Hence the two terms on the right-hand side of (4) must balance;

$$\partial\xi_x/\partial x \sim -i\lambda\xi_y. \quad (5)$$

This generates the ordering $\xi_y \sim \xi_x/\lambda$, $b_z \sim \xi_y/\lambda \sim \xi_x/\lambda^2$, when $\partial/\partial x \sim O(1)$.

We can formalize this ordering by expanding the variables ξ_x and ξ_y in a power series in ϵ, that is,

$$\xi_x = \xi_{x0} + \epsilon\xi_{x1} + \epsilon^2\xi_{x2} + \cdots \quad (6)$$

$$\xi_y = \xi_{y0} + \epsilon\xi_{y1} + \epsilon^2\xi_{y2} + \cdots \quad (7)$$

(where $\xi_{\alpha n} \sim O(1), \alpha = x, y$). The above ordering requires $\xi_{y0} = 0$, and at leading order

$$\frac{\partial \xi_{x0}}{\partial x} + i\lambda\epsilon\xi_{y1} = 0, \quad (8)$$

which suggests the ordering $\epsilon = 1/\lambda$.

2.2. Transversally Symmetric Alfvén Waves ($\lambda \sim \partial/\partial x \gg k_z$)

We can also consider orderings when both perpendicular wave variations occur on lengthscales much shorter than those parallel to the background field. This will be appropriate for some of the radially localized high-m waves discussed earlier. To illustrate this we consider $\partial/\partial x \sim \lambda$ and both $\gg k_z$. In this case (3) still implies $b_z \sim \xi_y/\lambda$ and hence the right-hand side of (4) must still be the balance of $\partial\xi_x/\partial x \sim -i\lambda\xi_y$. Now, however, both polarizations will be dominated by the leading order terms, that is, $\xi_{x0}, \xi_{y0} \neq 0$. Assuming λ still represents the largest magnitude in the system we can retain the ordering $\epsilon = 1/\lambda$. Strictly, this restricts the magnitude of the x variations to $\partial/\partial x \sim \lambda$ so that (6) and (7) still correctly describe the wave variations at every order.

3. Multiple-Timescales Analysis

In this section we use the asymptotic method of multiple-timescales to determine analytic wave solutions over timescales much longer than t. Following standard methods [e.g., *Bender and Orszag*, 1978], we define a long timescale $\sigma = \epsilon t$, with $\epsilon = 1/\lambda$, as suggested by (8) and treat the variables t and σ as independent. Multiple-timescales analysis allows the determination of the wave solutions as a function of both t and σ.

Combining (2) and (3) by eliminating b_z, we obtain

$$\frac{1}{\omega_A^2(x)}\frac{\partial^2 \xi_x}{\partial t^2} + \xi_x = \frac{1}{i\lambda}\frac{\partial}{\partial x}\left(\frac{1}{\omega_A^2(x)}\frac{\partial^2 \xi_y}{\partial t^2} + \xi_y\right). \quad (9)$$

It turns out that since $b_z \sim \xi_y/\lambda$ and $\partial\xi_x/\partial x + i\lambda\xi_y \approx 0$ for both the wave orderings discussed in sections 2.1 and 2.2, inserting the power series expansions (6) and (7), and substituting for the leading order (nonzero) component of ξ_y in terms of ξ_x on the right-hand side of (9) generates, in both cases, the leading order equation

$$\frac{1}{\omega_A^2(x)}\frac{\partial^2}{\partial t^2}(\xi_{x0} + \epsilon\xi_{x1} + \ldots) + \xi_{x0} + \epsilon\xi_{x1} + \ldots =$$
$$\epsilon^2\left\{\frac{\partial}{\partial x}\left[\frac{1}{\omega_A^2(x)}\frac{\partial^2}{\partial t^2}\left(\frac{\partial \xi_{x0}}{\partial x}\right) + \frac{\partial \xi_{x0}}{\partial x}\right]\right\} + O(\epsilon^3). \quad (10)$$

This equation describes both dominantly poloidal and more symmetric transverse Alfvén wave disturbances depending upon the magnitude of the x variations (i.e., whether $\lambda \gg \partial/\partial x$ or $\lambda \approx \partial/\partial x$, respectively).

To proceed, we rewrite the ξ_x expansion in (6) in terms of a multiple-timescales variable Φ, that is,

$$\xi_x(x,t) = \Phi_0(x,t,\sigma) + \epsilon\Phi_1(x,t,\sigma) + \ldots \quad (11)$$

and following standard techniques use the chain rule to substitute

$$\frac{\partial^2 \xi_x}{\partial t^2} = \frac{\partial^2 \Phi_0}{\partial t^2} + \epsilon \left(2 \frac{\partial^2 \Phi_0}{\partial t \partial \sigma} + \frac{\partial^2 \Phi_1}{\partial t^2} \right) + O(\epsilon^2). \quad (12)$$

This results in a hierarchy of equations in powers of ϵ, which can be solved to generate the wave solutions.

3.1. Zeroth-Order Solution

To leading order, we simply have the equation

$$\frac{1}{\omega_A^2(x)} \frac{\partial^2 \Phi_0}{\partial t^2} + \Phi_0 = 0 \quad (13)$$

which has the solution

$$\Phi_0(x,t,\sigma) = \Phi_0^+ + \Phi_0^- \equiv H_0^+(x,\sigma) \exp +i\omega_A(x)t + H_0^-(x,\sigma) \exp -i\omega_A(x)t. \quad (14)$$

The integration constants H_0^+ and H_0^- can, at this stage, be different functions of x and σ.

3.2. First Order Solution

Substituting the zeroth-order solution into (10) and retaining terms up to order ϵ we find

$$\frac{1}{\omega_A^2(x)} \frac{\partial^2 \Phi_1}{\partial t^2} + \Phi_1 = \left(-\frac{2}{\omega_A^2(x)} \frac{\partial^2 \Phi_0^+}{\partial t \partial \sigma} - 2 \frac{i\omega_A'^2(x)}{\omega_A(x)} \sigma \Phi_0^+ - 2 \frac{i\omega_A'^2(x)}{\omega_A(x)} \sigma^2 \frac{\partial \Phi_0^+}{\partial \sigma} \right) + \left(-\frac{2}{\omega_A^2(x)} \frac{\partial^2 \Phi_0^-}{\partial t \partial \sigma} + 2 \frac{i\omega_A'^2(x)}{\omega_A(x)} \sigma \Phi_0^- + 2 \frac{i\omega_A'^2(x)}{\omega_A(x)} \sigma^2 \frac{\partial \Phi_0^-}{\partial \sigma} \right) \quad (15)$$

where the x derivatives have been calculated according to

$$\frac{\partial \Phi_0^\pm}{\partial x} = \pm H_0^\pm(x,\sigma) i\omega_A'(x) t \exp \pm i\omega_A(x)t + H_0^{\pm\prime}(x,\sigma) \exp \pm i\omega_A(x)t \quad (16)$$

and where $a' = \partial a / \partial x$. We look for the σ dependence of $H_0^\pm$ so that Φ_1 is not secularly driven by Φ_0 (i.e., so that the first-order oscillator on the left-hand side of (15) is not resonantly driven at $\omega_A(x)$). This ensures that the asymptotic expansion orderings of $\Phi_0, \Phi_1 \ldots$ with ϵ remain valid over the long timescale σ, rather than just the short timescale t, and generates a solvability condition whereby the right-hand side of (15) must equal zero.

Hence the poloidal Alfvén wave solvability condition is

$$\frac{\partial H_0^\pm}{\partial \sigma} + \sigma \omega_A'^2(x) H_0^\pm + \sigma^2 \omega_A'^2(x) \frac{\partial H_0^\pm}{\partial \sigma} = 0 \quad (17)$$

with the solution

$$\ln H_0^\pm = -\frac{1}{2} \ln(1 + \omega_A'^2(x)\sigma^2) + \ln G^\pm(x). \quad (18)$$

The constants of integration are determined by boundary conditions, for example, $G^\pm(x) = H_0^\pm(x, \sigma = 0)$, so that

$$H_0^\pm(x,\sigma) = \frac{G^\pm(x)}{(1 + \omega_A'^2(x)\sigma^2)^{\frac{1}{2}}}. \quad (19)$$

In (17) we have assumed $H_0^{\pm\prime}$ (i.e., $\partial/\partial x$) $\ll \lambda$, corresponding to the poloidal Alfvén wave case. When $H_0^{\pm\prime}$ is large, additional terms can be introduced into the solvability condition to take account of the increased magnitude of $G^{\pm\prime}(x)$. We consider the inclusion of these additional terms where necesssary when we compare our asymptotic solutions to numerical simulations in section 5.

The leading order toroidal solution is calculated from (8), so that

$$i\xi_y = -\frac{H_0^{+\prime}}{\lambda} \exp +i\omega_A(x)t - i\omega_A'(x)\sigma H_0^+ \exp +i\omega_A(x)t - \frac{H_0^{-\prime}}{\lambda} \exp -i\omega_A(x)t + i\omega_A'(x)\sigma H_0^- \exp -i\omega_A(x)t. \quad (20)$$

Wave fields initially oscillate $\sim \exp \pm i\omega_A(x)t$, and as time evolves, the initial coherent wave disturbance phase mixes in time whilst the wave amplitudes develop according to (14) and (20), with $H_0^\pm$ as given in (19).

3.3. Second- and Higher-Order Solutions

Second- (and higher-) order solutions can be found by continuing the multiple timescales analysis. The second-order solution gives a solvability condition for the σ dependence of Φ_1 and so on. Since higher-order solutions scale with powers of ϵ, they are relatively unimportant and become increasingly algebraically tedious to compute. Hence we do not present any higher-order solutions here.

When the envelope $G^\pm(x)$ is localized (as is typically the case for poloidal Alfvén waves in the magnetosphere), its gradients can form an important parameter which changes the features of even the first-order solution. For magnetospheric pulsations this behavior appears to be more important than the form of the higher-order solutions, and we discuss this in section 5.

4. Physical Wave Solutions

Physical Alfvén wave solutions can be calculated from the theory presented earlier by taking $\xi_x^P = Re(\xi_x)$ and $\xi_y^P = Re(\xi_y)$, where Re(a) means the real part of a. When comparing theory to observations, standing or propagating azimuthal phase variation generates wave solutions with differing polariszations. Since $H_0^{\pm\prime}(x,\sigma) \to 0$ as $\sigma \to \infty$, both poloidal and toroidal

initial wave disturbances decay as they drive the additional toroidal wave (the second term on the right-hand side of (20)). Both azimuthally standing and propagating solutions asymptote toward decoupled toroidal oscillations at the local natural Alfvén frequency $\omega_A(x)$ in accord with the asymptotic state predicted by *Radoski* [1974].

4.1. Azimuthally Standing Waves

In this case the waves are torsional waves consisting of oscillating twisted flux tubes standing in y and is produced by setting $H_0^+ = H_0^- = H_0/2$ and $G^+ = G^- = G/2$, so that

$$\begin{aligned} \xi_x^P &= \mathrm{Re}(H_0(x,\sigma)\cos\omega_A(x)t\exp i\lambda y\sin k_z z) \\ \xi_x^P &= H_0(x,\sigma)\cos\omega_A(x)t\cos\lambda y\sin k_z z \end{aligned} \tag{21}$$

$$\xi_y^P = \sin\lambda y\sin k_z z\times \left(H_0\omega_A'\sigma\sin\omega_A(x)t - \frac{H_0'}{\lambda}\cos\omega_A(x)t\right)$$

$$\xi_y^P = -I_0(x,\sigma)\cos(\omega_A(x)t+\phi)\sin\lambda y\sin k_z z \tag{22}$$

where

$$I_0 = (H_0^2\omega_A'(x)^2\sigma^2 + H_0'^2/\lambda^2)^{\frac{1}{2}}$$

and

$$\phi = \tan^{-1}(H_0\omega_A'(x)\sigma\lambda/H_0').$$

The waves initially oscillate in phase, and in a medium where $\omega_A'(x)$ is negative (e.g., outside the plasmapause, where the local Alfvén frequency decreases with L shell), waves with negative λ will develop a clockwise polarization in time (when viewed in the direction of B_0). Numerical solutions of this type were presented by *Mann and Wright* [1995, Figure 5] and are considered further in section 5.

4.2. Azimuthally Propagating Waves

Poloidal Alfvén waves driven by the drift-bounce resonance mechanism will have azimuthal phase propagation, since they are driven by maintaining constant phase with westward drifting, mirroring energetic protons. Such solutions are generated by setting $H_0^+ = 0$ and $H_0^- = H_0$, that is, $G^+ = 0$ and $G^- = G$, which yields ξ_x^P of the form

$$\begin{aligned} \xi_x^P &= \mathrm{Re}(H_0\exp(-i\omega_A(x)t)\exp i\lambda y\sin k_z z) \\ \xi_x^P &= H_0\cos(\omega_A(x)t-\lambda y)\sin k_z z. \end{aligned} \tag{23}$$

Again using (5) generates the associated toroidal signal

$$\xi_y^P = \sin k_z z\times \left[H_0\omega_A'(x)\sigma\cos(\omega_A(x)t-\lambda y) + \frac{H_0'}{\lambda}\sin(\omega_A(x)t-\lambda y)\right]$$

$$\xi_y^P = I_0\sin(\omega_A(x)t-\lambda y+\phi)\sin k_z z. \tag{24}$$

In this case the initial (traveling) ξ_x^P and ξ_y^P are in quadrature. For waves outside the plasmapause with negative λ (westward phase propagation), they are polarized clockwise (viewed in the direction of B_0) poleward and anticlockwise equatorward of the peak in $G(x)$. Wave evolution drives an additional toroidal component in phase with the initial poloidal wave, and this rotates the polarization ellipses clockwise (viewed in the direction of B_0) when both $\omega_A'(x)$ and λ are negative.

5. Comparison Between Asymptotic and Numerical Results

Here we compare our analytic solutions to numerical results for azimuthally standing waves calculated using the code described by *Mann and Wright* [1995] (see also *Mann et al.* [1995]). The Alfvén speed variation in this model is described by

$$v_A^{-2}(x) = A^2 - B^2\cos(\pi x) \tag{25}$$

where we have chosen $A^2 = 1$ and $B^2 = 0.2$. To incorporate the dependence of the wave solutions on the envelope of the disturbance, we consider $G(x)$ of the form

$$G(x) = \exp(-(x-x_r)^2/x_w^2). \tag{26}$$

The code describes azimuthally standing waves, and we consider waves which are initially at rest and linearly incompressible so

$$\frac{\partial\xi_x(x,t=0)}{\partial x} + i\lambda\xi_y(x,t=0) = 0 \tag{27}$$

(hence $G(x)$ also determines the initial toroidal field).

The relative magnitudes of λ and G' determine the initial toroidal and poloidal amplitudes, being dominantly poloidally polarized for $\lambda > G'$, toroidally for $\lambda < G'$, and nearly symmetrically polarized when $\lambda \sim G'$. Assuming that $\partial/\partial x \sim x_w^{-1}$, the wave amplitudes will be approximately equal when $x_w = \lambda^{-1}$. Since the initial wave profiles are Gaussian we find that the x integrated energies E_p ($=\int e_p dx$) and E_t ($=\int e_t dx$) (where $e_{p,t} = \rho\dot{\xi}_{x,y}^2/2 + b_{x,y}^2/2\mu_0$) of the initial poloidal and toroidal fields have the ratio $E_p/E_t = \lambda^2 x_w^2$ and hence are equal when $x_w = \lambda^{-1}$.

We consider two particular examples, the first representing a poloidal Alfvén wave having large λ (typical of afternoon poloidal Alfvén waves) and the second having smaller λ (yet still $\gg k_z$) where at $t = 0$, ξ_x and ξ_y have similar magnitudes and represent more symmetric transverse waves. In each case we varied x_w as a parameter; its magnitude relative to $1/\lambda$ determined the resultant wave behavior. All numerical calculations are completed in a box having width $L_X = 5\ R_E$, with $k_z = 1.93$ to approximate second harmonic waves on field lines of length $2.5L\ R_E$ at $L = 6.5$.

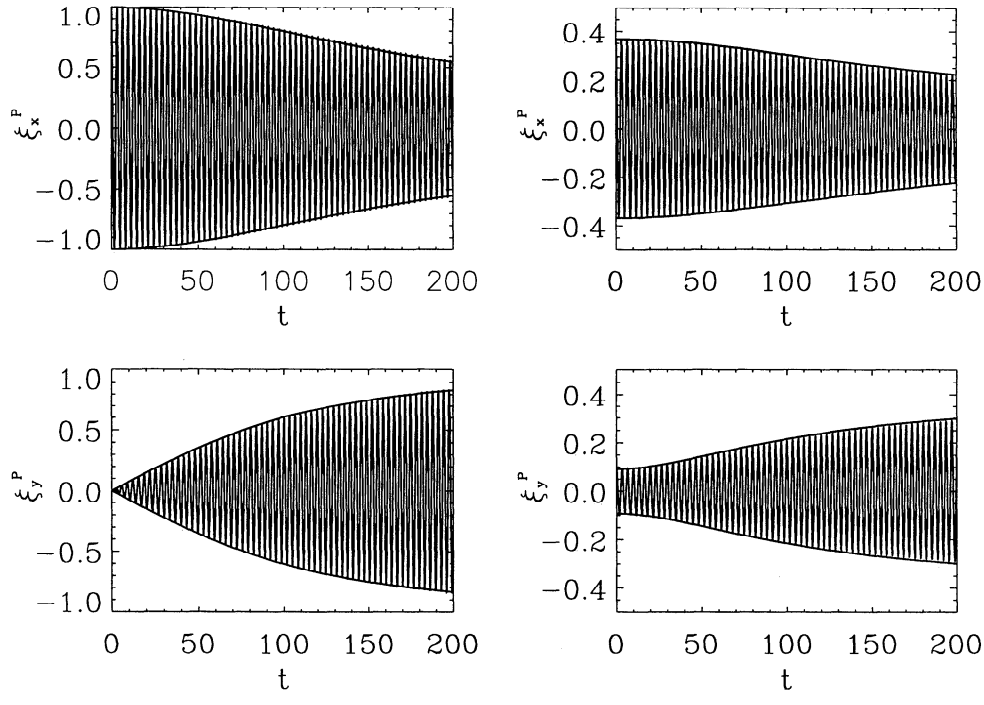

Figure 1. The physical plasma displacements ξ_x^P and ξ_y^P as a function of time for $x_w = 0.1$, $\lambda = 80$. The oscillating fields are generated numerically and overplotted are the asymptotic envelopes H_0 and I_0 calculated using (19). (left) Position $x = x_r = 0.5$ and (right) position $x = x_r + x_w = 0.6$.

5.1. Poloidal Alfvén Waves

We take $\lambda = 80$ to approximate afternoon poloidal Alfvén waves with $m \sim 100$, and Figure 1 shows numerical time series for ξ_x^P and ξ_y^P at $x = x_r$ and $x = x_r + x_w$, for $x_w = 0.1$ (i.e., a magnetospheric width $2x_w = 1\ R_E$). Overplotted are the leading order multiple-timescale envelopes H_0 and I_0 calculated on the basis of (19). The agreement between the multiple timescales and the numerical solutions is excellent. This represents a case where $\lambda x_w = 8$ and corresponds to initial conditions which are dominantly poloidally polarized. The agreement between the analytical and numerical solutions increases as λx_w increases (not shown).

To further illustrate poloidal Alfvén wave behavior, Figure 2 shows the numerical time evolution of E_p and E_t for $x_w = 0.25, 0.1$, and 0.025 corresponding to magnetospheric widths $2x_w = 2.5$, 1.0, 0.25 R_E, respectively, typical of observations. Even for the most localized waves the asymptotic polarization rotation from toroidal to poloidal remains a robust feature, and the solutions are accurately estimated using (19). Note that "the poloidal lifetime" (the time τ at which $E_t = E_p$) is approximately independent of x_w. Indeed, *Mann and Wright* [1995] showed $\tau \approx \lambda/\omega_A'(x)$ and that τ is determined to leading order by λ alone. (For the parameters employed in Figure 2 (and using the value of $\omega_A'(x = 0.5)$) predicts $\tau \approx 132$.)

5.2. Transversally Symmetric Alfvén Waves

We now take $\lambda = 20$ and consider initial wave fields with similar toroidal and poloidal amplitudes. This approximates $m \sim 25$ and could be applicable to Pgs.

As we discussed earlier, for more symmetric large-λ Alfvén wave disturbances we can retain additional terms in the solvability condition which arise from the x variation of the envelope of the waves, that is, H_0' and

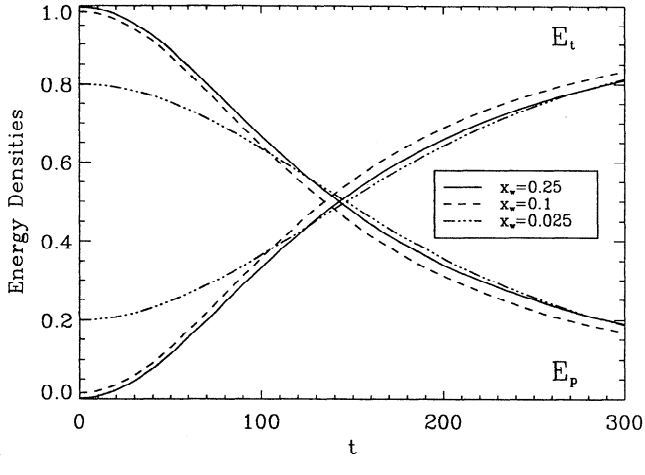

Figure 2. Time evolution of the x integrated poloidal and toroidal energy densities E_p and E_t for $x_w = 0.25$, 0.1, and 0.025 when $\lambda = 80$.

H_0''. Assuming that the Alfvén frequency gradients are of a lower order than the envelope variations, retaining the H_0 gradient terms gives the following solvability condition:

$$\frac{\partial H_0}{\partial \sigma} + \sigma \omega_A'^2(x) H_0 + \sigma^2 \omega_A'^2(x) \frac{\partial H_0}{\partial \sigma} - 2\epsilon^2 \frac{\omega'}{\omega} \frac{\partial H_0'}{\partial \sigma} - 2i\epsilon\omega'\sigma \frac{\partial H_0'}{\partial \sigma} - \epsilon^2 \frac{\partial H_0''}{\partial \sigma} - i\epsilon H_0'\omega' = 0 \quad (28)$$

where the first three terms are again those from (17). Assuming that the dominant H_0 gradients arise from variations in the wave envelope $G(x)$, substituting $H_0' = G'H_0/G$ and $H_0'' = H_0\left[(G'/G)' + (G'/G)^2\right]$ we find the modified solution

$$H_0^{\bullet}(x,\sigma) = \frac{G(x) f^{\frac{1}{2}}(x)}{\left(f(x) + \omega_A'^2(x)\sigma^2 - 2i\omega_A'(x)\sigma G'/\lambda G\right)^{\frac{1}{2}}}, \quad (29)$$

where $f(x) = 1 - (2G'\omega'/\omega G + G''/G)/\lambda^2$. Strictly, this solution should only be accurate when $G'/G \lesssim \lambda$ and $G''/G \lesssim \lambda^2$ so that the expansions (6) and (7) remain valid. Clearly, when the scale on which G varies on is much greater than the azimuthal wavelength, $f(x) = 1$ and the solution reverts to the poloidal Alfvén wave solution in (19).

In Figure 3 we show the numerical time series for ξ_x^P and ξ_y^P when $x_w = 0.2$, again at $x = x_r$ and $x_r + x_w$. Overplotted as solid curves are the multiple timescales envelopes caclulated from (19); overplotted as dot-dash curves are the envelopes calculated using the extra $G(x)$ gradient terms in (29). Both envelopes are in good agreement with the numerics, with that from (29) giving better agreement. The additional terms introduce a slight transfer of energy across the field lines, since where G' is large the poloidal solution decays faster than where it is small. Here $\lambda x_w = 4$ so that in terms of total energy the wave is still dominantly poloidal; however, the x and y variations are of a similar magnitude (i.e. $\partial/\partial x \sim \lambda$). In this case we might expect the H_0 gradient terms to be important - in good agreement with our results.

Further decreasing the radial width of the pulsations generates initial conditions which are increasingly less poloidal. As λx_w decreases, the assumptions used to calculate the asymptotic solutions become increasingly less appropriate, since the waves are no longer clearly dominated by the scalength $2\pi/\lambda$. In Figure 4 we show the numerical time evolution of E_t and E_p for three values of $x_w \geq \lambda^{-1}$, when $\lambda = 20$. The qualitative trend of polarization rotation from poloidal to toroidal remains a robust feature of the wave evolution, and the concept of a finite poloidal Alfvén wave lifetime remains valid. Once $\lambda x_w < 1$ (i.e., $x_w < 0.05$), the initial wave conditions become dominantly toroidal rather than poloidal. In this case the monotonic exchange of energy from poloidal to toroidal waves polarizations ceases; the poloidal waves gaining energy at the expense of the toroidal ones over short timescales

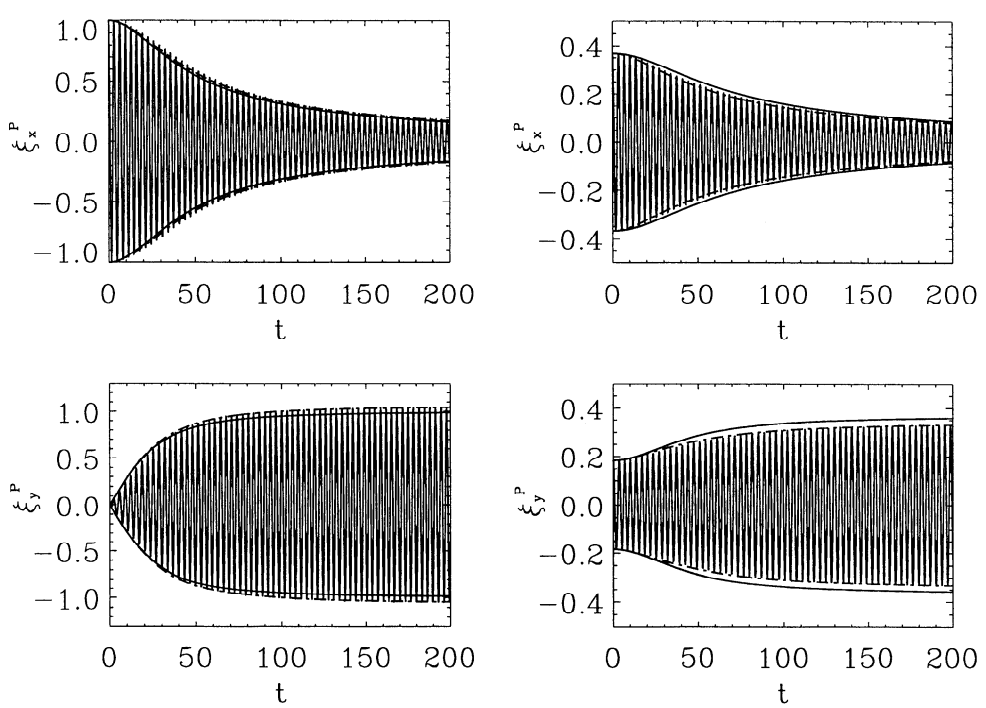

Figure 3. Displacements ξ_x^P and ξ_y^P versus t for $x_w = 0.2$, $\lambda = 20$. The numerical solution is plotted as the oscillatory solid line, the asymptotic solution from (19) is plotted as the solid envelope, and the asymptotics from (29) are plotted as the dot-dash envelope. (left) Position $x = x_r = 0.5$ and (right) position $x = x_r + x_w = 0.7$.

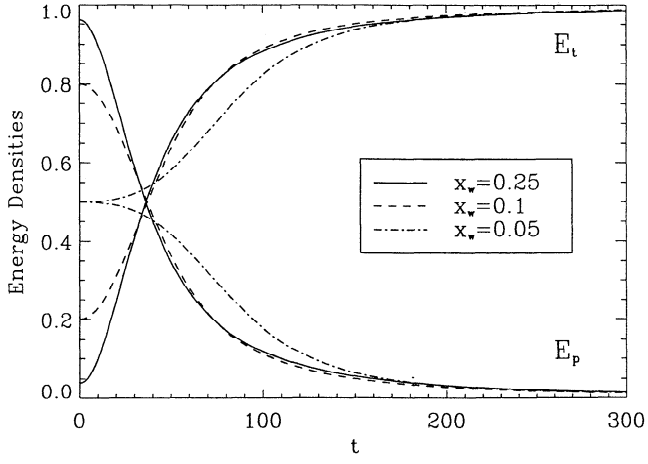

Figure 4. Time evolution of the x integrated poloidal and toroidal energy densities E_p and E_t for $x_w = 0.25$, 0.1, and 0.05 when $\lambda = 20$ ($\lambda x_w = 5$, 2, and 1, respectively).

before again approaching a purely toroidal asymptotic state (not shown).

Observations show magnetospheric high-m waves to have widths $\sim 0.2 - 3.1\ R_E$, typically $\sim 1\ R_E$. Our asymptotic solutions should be very accurate for waves with $m \sim 100$, and whilst there may be some small departure for the narrowest wave envelopes when m is smaller, for example, ~ 25 (for Pgs), the asymptotic solutions should still be qualitatively correct. In general, waves with a dominantly poloidal polarization should display behavior in agreement with section 3. For all values of x_w, waves with $\lambda \gg k_z$ ultimately have a time asymptotic state consisting of purely decoupled toroidal oscillations.

6. Discussion

The time-dependent poloidal Alfvén wave polarization rotation which we have demonstrated here occurs naturally for initially poloidally polarized high m waves oscillating in radially inhomogeneous plasmas. The physical reason for the polarization changes can be understood in terms of the leading order incompressibilty of the waves as follows. In linear theory the compression of a cold plasma can be identified with b_z, which is zero to leading order for waves with large azimuthal wavenumbers. From this leading order incompressibility it follows that adjacent field lines can oscillate nearly independently of each other and hence in an inhomogeneous medium will phase mix and only experience weak perpendicular dispersion. In a time-dependent model, phase mixing increases the radial wavenumber (k_x) in time, so that as phase mixing proceeds the leading order poloidal amplitude decreases whilst the toroidal amplitude increases. This generates the asymptotic solution we presented in section 3.

Our solutions are applicable to the evolution of undriven waves, as studied by, for example, *Ding et al.* [1995]. In the magnetosphere, poloidal Alfvén waves may be driven by drift-bounce resonance, and in this sense our results may be more applicable to situations where the waves are no longer being driven. During the driven phase of the waves, the full solution will be a combination of the undriven (or homogeneous) solution described in this paper and the "particular integral" (or inhomogeneous) solution. Many features of the driven solution can be dominated by the homogeneous part of the solution, as is the case for low-m Alfvén resonances. Moreover, we can gain a qualitative insight into the likely behavior of the full driven poloidal Alfvén wave fields by considering the driven wave fields as a summation over repeatedly excited evolving solutions to the undriven initial value problem, such as those presented in this paper. This thought experiment is equivalent to a "Green's function" solution where the inhomogeneous solution is constructed from a sum (or integral) of functions that are formed from the homogeneous solutions in a piecewise continuous fashion.

For our polarization rotation to be able to be observed in data, the wave evolution must occur on a timescale quicker than ionospheric dissipation. For 100s period, second harmonic poloidal Alfvén waves in a dipole field at $L = 6.5$ we estimate poloidal lifetimes τ (the time for the toroidal amplitude to grow to equal the (decreasing) poloidal one [see *Mann and Wright*, 1995]) of ~ 2.6 and ~ 8.5 periods for $m \sim 30$ and 100, representing typical Pgs or afternoon Pc4s, respectively [see G. Chisham et al., 1996, A statistical study of giant pulsation (Pg) latitudinal polarization and amplitude variation, submitted to *Journal of Geophysical Research*]. Using the results of *Newton et al.* [1978], we estimate day and night undriven ionopsheric decay times of ~ 15 and ~ 2 periods, respectively. Consequently, dayside observations should show clearer evidence for wave evolution with the heavy damping at night expected to show wave signatures more characteristic of the waves driving mechanism rather than any subsequent evolution.

Satellite observations by *Hughes and Grard* [1984] show unusual polarization intervals which might be the result of wave evolution, although it is difficult to unravel spatial and temporal changes using satellite data. Since high-m afternoon Pc4 waves are believed to be screened from ground-based magnetometers, maybe the best way to observe poloidal Alfvén wave evolution would be using two-dimensional ionospheric flows deduced from radars such as SABRE [*Nielson et al.*, 1983]. The velocity vectors would be expected to show latitude-dependent frequencies, combined with a power transfer from poloidal to toroidal oscillations. Because of the action of the driving mechanism, the L-dependent oscillation frequency (a signature of phase mixing) might be more apparent at the end of a temporal wave packet, once the waves are no longer being driven. Since poloidal Alfvén waves with latitude-dependent frequencies have been observed pre-

viously in satellite data [e.g., *Engebretson et al.*, 1988], we believe the poloidal Alfvén wave evolution we have demonstrated here may be observable using radar.

7. Conclusions

In this paper we have presented time-dependent analytic poloidal Alfvén wave solutions, applicable to high-m waves in the magnetosphere, by using the asymptotic method of multiple timescales. Our solutions show the leading order phase mixing ($\exp i\omega_A(x)t$) behavior expected for Alfvénic disturbances oscillating in radially inhomogeneous plasmas, and analytically reproduce the polarization rotation from poloidal to toroidal seen numerically by *Mann and Wright* [1995].

We investigated the importance of the observed radial localization of poloidal Alfvén waves in determining their time-dependent behavior by comparing our analytic solutions to numerical ones. Our asymptotics produced highly accurate solutions when $\lambda \gg k_x, k_z$, that is, for initial conditions comprising strongly poloidal Alfvén waves (applicable to $m \sim 100$ afternoon poloidal Alfvén waves). Reducing the waves radial widths so that $k_x, \lambda \gg k_z$ (representing more symmetric transverse Alfvén wave disturbances) required the inclusion of extra terms involving gradients in the waves radial envelope to maintain agreement between analytic and numerical solutions. Reducing the radial widths further, so that the waves were no longer initially poloidal, reduced the accuracy of the asymptotics. Numerically, in this case the toroidal amplitude grew at the expense of the poloidal one at early times. However, all the high-λ initial conditions (regardless of radial localization) evolved toward the same time asymptotic state, namely, purely decoupled toroidal oscillations at the local Alfvén frequency $\omega_A(x)$. The interpretation of observations of high-m waves in the magnetosphere should take account of this evolution.

Acknowledgments. This work was carried out while A.N.W. was supported by a PPARC Advanced Fellowship. I.R.M. was supported by a PPARC studentship at the University of St. Andrews, and a PPARC postdoctoral position via grant GR/K94133 at QMW.

The Editor thanks two referees for their assistance in evaluating this paper.

References

Anderson, B. J., M. J. Engebretson, S. P. Rounds, L. J. Zanetti, and T. A. Potemra, A statistical study of pulsations observed by the AMPTE/CCE magnetic fields experiment, 1, Occurrence distributions, *J. Geophys. Res.*, *95*, 10,495, 1990.

Anderson, B. J., T. A. Potemra, L. J. Zanetti, and M. J. Engebretson, Statistical correlations between Pc 3-5 pulsations and solar wind/IMF parameters and geomagnetic indices, in *Physics of Space Plasmas (1990)*, vol. 10, *SPI Conf. Proc. Reprint Ser.*, edited by T. Chang, G. B. Crew, and J. R. Jasperse, p. 419, Scientific, Cambridge, Mass., 1991.

Bender, C. M., and S. A. Orszag, *Advanced Mathematical Methods for Scientists and Engineers*. McGraw-Hill, New York, 1978.

Chan, A. C., X. Mengfen, and L. Chen, Anisotropic Alfvén ballooning modes in Earth's magnetosphere, *J. Geophys. Res.*, *99*, 17,351, 1994.

Chen, L., and A. Hasegawa, A theory of long-period magnetic pulsations, 1, Steady state excitation of field line resonance, *J. Geophys. Res.*, *79*, 1024, 1974.

Chen, L., and A. Hasegawa, On magnetospheric hydromagnetic waves excited by energetic ring current particles, *J. Geophys. Res.*, *93*, 8763, 1988.

Chen, L., and A. Hasegawa, Kinetic theory of geomagnetic pulsations, 1, Internal excitations by energetic particles, *J. Geophys. Res.*, *96*, 1503, 1991.

Chisham, G., Giant pulsations (Pgs): An explanation for their rarity and occurrence during geomagnetically quiet times, *J. Geophys. Res.*, *101*, 24,755, 1996.

Chisham, G., D. Orr, M. J. Taylor, and H. Lühr, The magnetic and optical signature of a Pg pulsation, *Planet. Space Sci.*, *38*, 1443, 1990.

Chisham, G., D. Orr, and T. K. Yeoman, Observations of a giant pulsation (Pg) across an extended array of ground magnetometers and on auroral radar, *Planet. Space Sci.*, *40*, 953, 1992.

Ding, D. Q., R. E. Denton, M. K. Hudson, and R. L. Lysak, An MHD simulation study of the poloidal mode field line resonance in the Earth's dipole magnetosphere, *J. Geophys. Res.*, *100*, 63, 1995.

Engebretson, M. J., L. J. Zanetti, T. A. Potemra, D. M. Klumpar, R. J. Strangeway, and H. Acuña, Observations of intense ULF pulsation activity near the geomagnetic equator during quiet times, *J. Geophys. Res.*, *93*, 12,795, 1988.

Engebretson, M. J., D. L. Murr, K. N. Erickson, R. J. Strangeway, D. M. Klumpar, S. A. Fuselier, L. J. Zanetti, and T. A. Potemra, The spatial extent of radial magnetic pulsation events observed in the dayside near synchronous orbit, *J. Geophys. Res.*, *97*, 13,741, 1992.

Glassmeier, K.-H., Magnetometer array observations of a giant pulsation event, *J. Geophys.*, *48*, 127, 1980.

Hasegawa, A., Drift mirror instability in the magnetosphere, *Phys. Fluids*, *12*, 2642, 1969.

Hillebrand, O., J. Munch, and R. L. McPherron, Ground-satellite correlative study of a giant pulsation event, *J. Geophys.*, *51*, 129, 1982.

Hughes, W. J., and D. J. L. Grard, A second harmonic geomagnetic field line resonance at the inner edge of the plasma sheet: GEOS 1, ISEE 1, and ISEE 3 observations, *J. Geophys. Res.*, *89*, 2755, 1984.

Hughes, W. J., and D. J. Southwood, An illustration of modification of geomagnetic pulsation structure by the ionosphere, *J. Geophys. Res.*, *81*, 3241, 1976.

Hughes, W. J., D. J. Southwood, B. Mauk, R. L. McPherron, and J. N. Barfield, Alfvén waves generated by an inverted plasma energy distribution, *Nature*, *275*, 43, 1978a.

Hughes, W. J., R. L. McPherron, and J. N. Barfield, Geomagnetic pulsations observed simultaneously on three geostationary satellites, *J. Geophys. Res.*, *83*, 1109, 1978b.

Kivelson, M. G., and D. J. Southwood, Resonant ULF waves: A new interpretation, *Geophys. Res. Lett.*, *12*, 49, 1985.

Kivelson, M. G., and D. J. Southwood, Coupling of global magnetospheric MHD eigenmodes to field line resonances, *J. Geophys. Res.*, *91*, 4345, 1986.

Kokubun, S., K. N. Erickson, T. A. Fritz, and R. L. McPherron, Local time asymmetry of Pc4-5 pulsations and associated particle modulations at synchronous orbit, *J. Geophys. Res.*, *94*, 6607, 1989.

Mann, I. R., and A. N. Wright, Finite lifetimes of ideal poloidal Alfvén waves, *J. Geophys. Res.*, *100*, 23,677, 1995.

Mann, I. R., A. N. Wright, and P. S. Cally, Coupling of magnetospheric cavity modes to field line resonances: A study of resonance widths, *J. Geophys. Res.*, *100*, 19,441, 1995.

Newton, R. S., D. J. Southwood, and W. J. Hughes, Damping of geomagnetic pulsations by the ionosphere, *Planet. Space Sci.*, *26*, 201, 1978.

Nielson, E., W. Guttler, E. C. Thomas, C. P. Stewart, T. B. Jones, and A. Hedburg, SABRE – A new radar auroral backscatter experiment, *Nature*, *304*, 712, 1983.

Poulter, E. M., W. Allan, E. Nielsen, and K.-H. Glassmeier, Stare radar observations of a Pg pulsation, *J. Geophys. Res.*, *88*, 5668, 1983.

Radoski, H. R., Highly asymmetric MHD resonances: The guided poloidal mode, *J. Geophys. Res.*, *72*, 4026, 1967.

Radoski, H. R., A theory of latitude dependent geomagnetic micropulsations: The asymptotic fields, *J. Geophys. Res.*, *79*, 595, 1974.

Rostoker, G., H. L. Lam, and J. V. Olson, Pc4 giant pulsations in the morning sector, *J. Geophys. Res.*, *84*, 5153, 1979.

Singer, H. J., W. J. Hughes, and C. T. Russell, Standing hydromagnetic waves observed by ISEE1 and 2: Radial extent and harmonic, *J. Geophys. Res.*, *87*, 3519, 1982.

Southwood, D. J., Some features of field line resonances in the magnetosphere, *Planet. Space Sci.*, *22*, 483, 1974.

Southwood, D. J., A general approach to low-frequency instability in the ring current plasma, *J. Geophys. Res.*, *81*, 3340, 1976.

Southwood, D. J., and M. G. Kivelson, Charged particle behavior in low-frequency geomagnetic pulsations, 2, Graphical approach, *J. Geophys. Res.*, *87*, 1707, 1982.

Southwood, D. J., J. W. Dungey, and R. J. Etherington, Bounce resonant interaction between pulsations and trapped particles, *Planet. Space Sci.*, *17*, 349, 1969.

Takahashi, K., and B. J. Anderson, Distribution of ULF energy ($f < 80$ mHz) in the inner magnetosphere: A statistical analysis of AMPTE CCE magnetic field data, *J. Geophys. Res.*, *97*, 10,751, 1992.

Takahashi, K., and R. L. McPherron, Standing hydromagnetic oscillations in the magnetosphere, *Planet. Space Sci.*, *32*, 1343, 1984.

Takahashi, K., R. W. McEntire, A. T. Y. Lui, and T. A. Potemra, Ion flux oscillations with a radially polarized transverse Pc5 magnetic pulsation, *J. Geophys. Res.*, *95*, 3717, 1990.

Takahashi, K., N. Sato, H. Lühr, H. E. Spence, and Y. Tonegawa, On the standing wave mode of giant pulsations, *J. Geophys. Res.*, *97*, 10,717, 1992.

Ian R. Mann, Astronomy Unit, Department of Mathematical Sciences, Queen Mary and Westfield College, University of London, Mile End Road, London, E1 4NS, U.K. (e-mail: I.Mann@qmw.ac.uk)

Alan W. Hood, Department of Mathematical and Computational Sciences, University of St. Andrews, St. Andrews, Fife KY16 9SS, Scotland. (e-mail: alan@dcs.st-and.ac.uk)

Andrew N. Wright, N.I.W.A., P.O. Box 14-901, Kilbirnie, Wellington, New Zealand. (e-mail: andy@dcs.st-and.ac.uk)

(Received July 16, 1996; revised September 19, 1996; accepted September 25, 1996.)